Araştırma Makalesi
Adıyaman Üniversitesi
Mühendislik Bilimleri Dergisi
23 (2024) 332-351

EXPERIMENTAL AND NUMERICAL ANALYSIS OF JET IMPINGING SOLAR AIR COLLECTOR WITH HEMISPHERICAL RIBS AND CIRCULAR TAPERED NOZZLE

İbrahim SANCAR[1*], Hüsamettin BULUT [2], Refet KARADAĞ [3]

[1]Adıyaman Üniversitesi, Teknik Bilimler Meslek Yüksek Okulu, Makine Bölümü, Adıyaman, 02040, Türkiye
[2]Harran Üniversitesi, Mühendislik Fakültesi, Makine Mühendisliği Bölümü, Şnlıurfa, 63290, Türkiye
[3]Adıyaman Üniversitesi, Mühendislik Fakültesi, Makine Mühendisliği Bölümü, Adıyaman, 02040, Türkiye
Geliş Tarihi/Received Date: 27.05.2024 Kabul Tarihi/Accepted Date: 11.06.2024 DOI: 10.54365/adyumbd.1490486

ABSTRACT
Studies are generally carried out on collector geometry and flow models in order to increase the thermal efficiency of solar air collectors (SACs), with are utilized in hot air production for various industrial and domestic applications. In jet impinging air collectors (JIPSAC), the geometric shape of the absorber plate and nozzle significantly affects the thermal performance. In this study, the plate with hemispherical ribs (HAP) and circular tapered nozzle (CTN) are proposed to increase the thermal efficiency of the jet impinging solar air collector. An experimental study was carried out to examine the effect of the jet flow air passing through the circular tapered nozzle hitting the hemispherical absorber plate on the thermal efficiency. CFD analysis of the created model was performed using Ansys Fluent 19.2 version. CFD results are compared with that of the experimental results. The contours of pressure and velocity streamlines are presented and discussed in order to help visualize the flow physics. From experimental and numerical analysis, it has been observed that the thermal efficiency of the jet impingement solar air collector using the plate with hemispherical ribs and circular tpared nozzle pair (HAP-CTN) provides a 12.33% increase on the average outlet temperature compared to the jet impinging solar air collector with flat absorber plate. In JIPSAC where HAP-CTN pair is used, in the experimental study conducted for the same combinations, the highest average efficiency of the collector was determined as 24.5% and the highest average collector outlet temperature 47.8 ºC at a mass flow rate of 0.0185 kg/s

Keywords: *CFD, circular tapered nozzle, jet impinging, hemispherical absorber plate, solar air collector.*

YARIM KÜRESEL PÜRÜZLÜ YUTUCU PLAKALI VE DAİRESEL KONİK NOZULLU JET ÇARPMALI HAVALI GÜNEŞ KOLLEKTÖRÜNÜN DENEYSEL VE SAYISAL ANALİZİ

ÖZET
Çeşitli endüstriyel ve evsel uygulamalar için sıcak hava üretiminde kullanılan havalı güneş kollektörlerinin (SAC) termal verimliliğini arttırmak için genellikle kollektör geometrisi ve akış modelleri üzerine çalışmalar yapılmaktadır. Jet çarpmalı hava kollektörlerinde (JIPSAC) yutucu plaka ve nozulun geometrik şekli, ısıl performansı önemli bir ölçüde etkilemektedir. Bu çalışmada jet çarpmalı havalı güneş kollektöründe ısıl verimliliğini artırmak için yarı küresel yüzeyli emici plaka (HAP) ve dairesel konik nozul (CTN) çifti önerilmiştir. Dairesel konik nozuldan geçen jet akışlı havanın yarım küre şekilli absorber plakaya çarpmasının ısıl verime etkisini incelemek için deneysel çalışma yapılmıştır. Modelin Ansys Fluent 19.2 versiyonu kullanılarak CFD analizi yapılmıştır. CFD sonuçları deneysel sonuçlar ile karşılaştırılmıştır. Akış fiziğini görselleştirmeye yardımcı olmak için basınç ve hız akım çizgilerinin konturları sunulmuş ve tartışılmıştır. Deneysel ve sayısal analizlerden, yarı küresel emici plaka ve dairesel konik nozul çifti (HAP-CTN) kullanılan jet çarpmalı havalı güneş kollektörünün ısıl verimliliğinin, düz yutucu plakalı jet çarpmalı havalı güneş kollektörüne kıyasla ortalama çıkış sıcaklığı üzerinde % 12.33 lük bir artış sağladığı görülmüştür. HAP-CTN çifti kullanılan JIPSAC' da aynı kombinasyonlar için yapılan deneysel çalışmada kollektörün en yüksek ortalama verimi, 0.0185 kg/s kütlesel debide % 24.5 ve en yüksek ortalama kollektör çıkış sıcaklığı 47.8 ºC olarak tespit edilmiştir.

Anahtar Kelimeler: *Hesaplamalı akışkan dinamiği, dairesel konik jet, jet çarpma plakası, yarım küre yutucu plaka, havalı güneş kollektörü*

e-posta1 : isancar@adiyaman.edu.tr ORCID ID : https://orcid.org/0000-0003-0282-6562 (Corresponding Author)
e-posta2 : hbulut@harran.edu.tr ORCID ID : https://orcid.org/0000-0001-7123-1648
e-posta3 : rkaradag@adiyaman.edu.tr ORCID ID : https://orcid.org/0000-0001-9120-2764

1. Introduction

Efficient renewable energy technologies are started to be investigated in academic studies due to the growing worldwide energy demand, the quick depletion of fossil fuel resources, and the rise in environmental pollutants caused by combustion. Solar energy is the most readily available, least expensive, practical, safe, sustainable, and clean energy source among the renewable energy sources. To benefit from solar energy, SAC have industrial and non-industrial application areas such as space heating, greenhouse heating, industrial plant drying.

Since SACs generally have low efficiency, some geometric studies have been carried out in order to regularize the flow and increase heat transfer by eliminating flow-baring geometries in the flow channel.

There is sufficient research on the absorber plate on SAC, roughness, fins and flow pattern in the air duct. To improve solar irradiance and increase collector efficiency, numerous researchers have investigated changing the absorber channel/plate shape to increase the rate of heat transfer by convection. Due to the increased convective SAC efficiency and heat transfer coefficient, jet impact plate solar air collectors (JIPSAC) have recently begun to be used in hot air production, and academic research has been concentrated in this direction.

There are many valuable studies that performance analysis using fins, deflection plates, corrugated absorber plates, grooved plates, rough, smooth plates and jet impinging in solar air collectors [1-10]. Dong et al. [11] Simulations stated that the use of grooved absorber plate increased the convective heat transfer coefficient by 1.8 to 2.3 times. Tuncer et al. [12] experımental studıes usıng plate shahs with perforated partitions were carried out. According to numerical findings, the use of perforated screens in vertical SAC ıncreased thermal effıcıency. According to experimental research, a modified v-groove SAC has a higher efficiency than a flat SAC, and a v-groove perforated jet absorber SAC has a higher efficiency than SACs with a regular v-groove absorber surface. [13]. By Farzan et al. [14] designed and experimentally analyzed a new type of SAC consisting of perforated metal plate and asphalt for building heating applications.

Experimental studies have revealed that cross-grooved channels outperform straight SACs by a large margin. In study to examine how the groove angle affects heat transport, the temperature rise is larger when using corrugated absorber plates [15-16]. A group of researchers conducted an experimental study on how V-shaped ribs with angles of 30°, 45°, and 60° in a rectangular channel affect the results. It was found that the efficiency index for the 45° ribbed channel was maximum for widely spaced ribs [17-19]. Elshafei et al. [20] Experimentally investigated the heat transfer and pressure loss in a channel with V-type corrugated top and bottom plates for various tilt angles. It was determined that an increase in wavy angle leads to more fluid recirculation, greater swirl flow intensity, and a larger surface area in the corrugation troughs, and as a result, the Nusselt number also rises.

In the experimental research conducted by Pehlivan et al. [21] the effect of forced convection on heat transfer for various inclined corrugated channels was examined. The impact of variables like groove height and slope angle on thermal efficiency has been the subject of several experimental investigations [22-26]. They suggested that the inclination angle and channel height of the V-groove channel have a significant effect on the friction coefficient and heat transfer [27-28]. According to analysis by Salman et al. [29] 74% and 70% of the thermal and effective efficiencies were attained when air jet impingement was performed on a heated surface with a roughness of dimple shape. Zhu et al. [30] conducted an experimental investigation to examine the decrease in pressure and thermal characteristics of a SAC that uses evacuated tubes and flat micro-heat pipe arrays under different airflow rates and seasons. According to reports, pressure drop in a SAC was achieved in the range of 16-24 Pa. Experimentally examined the effect of Nusselt number and friction factor on jet impingement solar air heater performance and the relationship between Nusselt number and friction factor [31].

Numerical and experimental study was conducted to study the effect of slot jet impingement on concave plates with varying surface curvature of the target distance of the nozzle in turbulent flow

environment [32-35]. They carried out experimental studies to analyze jet impingement cooling depending on Reynolds number, surface roughness, jet-plate separation, and jet geometry [36-39]. Culun et al.[40] examined the effect of design factors such as the shape and arrangement of jet holes, the density of jets moving in both aperture and flow direction, and jet-to-jet spacing and jet-to-target plate distance on SAC. It is concluded that square jet impingement has better performance than circular jet impingement. Cross-grooved absorber plate and jet ımpact factor Aboghrara et al.[41] It was put forward by. A significant improvement in thermal performance was discovered when comparing jet ımpacted corrugated SAC with flat plate SAC. The practical and theoretical examination of unglazed corrugated solar collectors with jet impingement were carried out by Belusko et al. [42]. It was shown that adding jet impingement can boost thermal efficiency by up to 21% while just slightly increasing pressure drop.

In experımental studıes studied the effect of jet impingement on different profiles of corrugated plates over a range of Reynolds numbers and jet-to-target plate distances. A thermal performance of 11.4 was achieved as compared to the base case [43-44]. On the other hand it was observed that the friction factor increased by approximately 9 times, resulting in a 7% improvement in efficiency. With the fintype geometry jet plate, an improvement of 6-16% was achieved. With the conical protruding jet impact plate, efficiency increased by 13.53% [45-46].

In experiments conducted by some researchers on SAC with jet impact plates to increase heat transfer, the effect of structural modifications such as inter-plate distances, jet hole diameters, and locations of jet holes were investigated. It has been reported collector efficiency in the range of 55.79 - 78% in modifications such as Multiple protrusions on a corrugated absorber plate spring barriers dimples on the absorber surface, transverse ribs on the absorber plate, etc.[47-53]. Metzer et al. [54] investigated the heat transfer parameters for two-dimensional jet arrays impinging in a plane parallel to the jet orifice plate.

Recent academic studies have focused on CFD analysis of jet impact plate SACs. The most obvious changes in these studies are the jet nozzle geometry and the surface geometry of the absorber plate hit by the jet flow.

Song et al. [56] looked into how the perforation plate affected the efficiency of PV SAC with baffles using a CFD technique. Furthermore, they discovered that M-SAC has a greater pressure drop than S-SAC. To assess the effectiveness of aluminum cans as absorber plates, Tan et al. [57] conducted an empirical and computer study. In the study conducted by Kumar et al. [58], the normal double pass SAC was modeled using a variety of CFD simulation tools. CFD and conducted an empirical analysis of a SAC with a ribbed and dimpled surface. Through CFD research, developed a new hybrid SAC design that combines triple depth v-groove SAC with parallel flow v-groove SAC. They have compared the numerical results with the experimental results of the parallel-flow v-grooved SAC (PFVSAC) and triple-flow v-grooved SAC (TFVSAC). [59–61]

Because of its increased convective SAC's efficiency and coefficient of heat transfer, jet impingement plate solar air collectors (JIPSAC) have become increasingly popular in hot air supply recently.

Considering that the V-shaped rib performance study demonstrated a greater pressure drop, Kumar et al. [62] changed the V-shape's sharp trailing edge to a flat arc shape and performed a computational analysis for different Re values between 6000 and 18000 while maintaining a constant heat flux condition of 1000 W/m^2. From 0.0299 to 0.0426 and from 0.333 to 0.666, respectively, the relative height of the roughened surface and relative angle (angle/90) were changing. The simulation made use of the RNG k-ε turbulent model. Because only conduction transfers heat, the CFD findings showed that Nu values were comparatively lower near the ribs. The introduction of recirculation zones, which encouraged fluid mixing and subsequently raised the heat transfer rate, is what caused these values to be higher immediately upstream and downstream of each rib. It was determined that the greatest effective thermal performance improvement over the bare plate was around 1.7 times.

Using a roughened absorber plate with rib grit, it was discovered that ribs with a 58-degree inclination transport 30% more heat than smooth SAC. Boulemtafes-Boukadoum et al. performed numerical analysis of SAC with transverse rectangular ribs absorber plate. CFD (computational fluid dynamics) research was carried out to compare sawtooth-shaped non-uniform rib roughness with circular, square and trapezoid-shaped uniform cross-section transverse ribs. Maximum nusselt number enhancements for sawtooth and trapezoidal rib-roughened ducts were 1.78 and 1.50, respectively [63-65].

Gawande and associates [66] Utilizing right-angled triangular ribs and synthetic roughness on the absorber plate, a discrete, two-dimensional programmed fluid dynamics (CFD) analysis of the Solar air chamber was carried out. Singh et al. [67] investigated the friction factor and Nusselt number of a solar air heater channel that was roughened with sawtooth ribs of non-uniform cross-section numerically.

A 2D CFD analysis was conducted using Ansys Fluent to assess the thermal performance of a novel hyperbolic ribbed SAC and carried out numerical simulations on their SAC and compared 3D results with 2D results and not found any considerable differences [68]. Kumar et al. [69] calculated the exergetic efficiency of a SAC using analytical methods on JIPSAC. A studie carried out computational modelling for cases of different geometric on flat plate and phase change material [70].

In the study conducted by Yadav et al.[71] similar to our present study, the heat transfer behavior of a solar air heater with a multiplying jet absorber plate was examined with a 3D-Computational fluid dynamics (CFD) simulation RNG kε turbulence model using ANSYS-18.1. A flat cylindrical jet nozzle was used in the study. The study's findings showed that, in comparison to standard solar air heaters, there was a maximum heat transfer increase of 7.58 and a friction factor penalty of 9.01 times. A numerical analysis is carried out on the heat transfer characteristics of a special SAC design with jet impinging plate through circular tapered nozzles using CFD simulations [72]. Re values of 14300 and 2900 yield the best thermal efficiency (91.25%) and energy efficiency (3.55%). Reynolds number (Re) was changed from 3500–17500 while keeping solar radiation at 1000 W/m² in a 3D CFD model with a cylindrical jet through that was built and simulated with a mass flow rate range of 0.0104–0.0524 kg/s [73].

Parameters and configurations such as using inclined jet impingement [74-78], microjet impingement for Re variation from 3000 to 16000 in a solar air collector with jet impingement compared to flat absorber plate collectors [79] have been tested.

In the same parallel flow jet impingement air solar collector, an increase in the outlet temperature of up to 15.5 °C was observed depending on pitch-hole diameter of jets. In studies where the Nusselt number and friction factor were improved, it was observed that there were 37-48% improvements in maximum thermo-hydraulic performance. Collector efficiency in the range of 55.79 - 78% has been reported in modifications such as absorber plates with different geometries [80-84]

This study focuses on the experimental and numerical analysis of Solar Air Collectors Using Hemispherical Absorber Plate and Circular Tapered Nozzle Pair (HAP-CTN-JIPSAC), unlike Solar Air Collectors using only Circular Conical Nozzle (CTN-JIPSAC).

2. CFD modelling of HAP-CTN-JIPSAC

Computational fluid dynamics (CFD) simulation of the 3D-model using a circular tapered nozzle was performed using the ANSYS-19.2 version with RNG kε turbulence model.

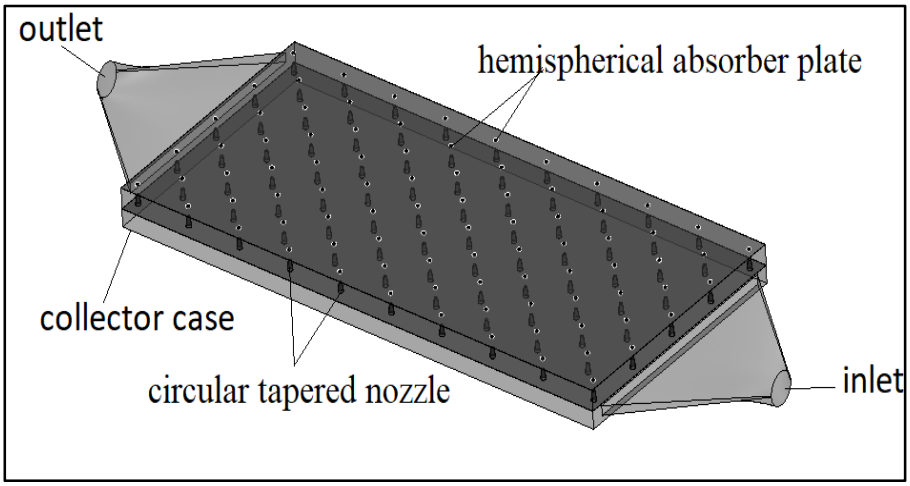

Fig. 1. Section views of HAP-CTN-JIPSAC

2.1. CFD domain of HAP-CTN-JIPSAC.

The sectional view of the solar air collector using hemispherical absorber plate and circular tapared nozzle pair and the isometric view of the hemispherical rib and circular tapared nozzle are given in fig. 1 and 2 It consists of two parallel flow regions with a jet impinging plate placed between them. Fig. 3 shows the schematic view of HAP-CTN-JIPSAC. The flow passing through the lower channel passes through nozzles placed at right angles and hits the hemispherical absorber plate. Here, the heated air leaves the collector parallel to the lower channel and in the same direction. Absorber plate, jet plate material and used as working fluid air characteristics are given in Table 2. Conical tapared nozzles are glued concentrically at the points drilled in the given dimensions on the rectangular cross-section sheet metal plate measuring 1860x980x1 mm. The hemispherical ribs are shaped with the help of a press on the absorber plate, exactly corresponding to the jet nozzles.

2.2. Assumptions

Several presumptions are established in order to establish the framework for the model's CFD analysis. These presumptions are:

1. JIPSAC has a constant heating effectiveness.
2. It was considered that the sky was a matte, black, dull object.
3. Collector case assumed to be fully insulated.
4. It is assumed that all working air temperatures in the air ducts are uniform.
5. It was thought that the air's temperature merely varied according to the direction of movement.
6. The holes of jet plate are tapered nozzle.
7. There is very little temperature loss in the bottom plate, absorber plate, and glass cover.

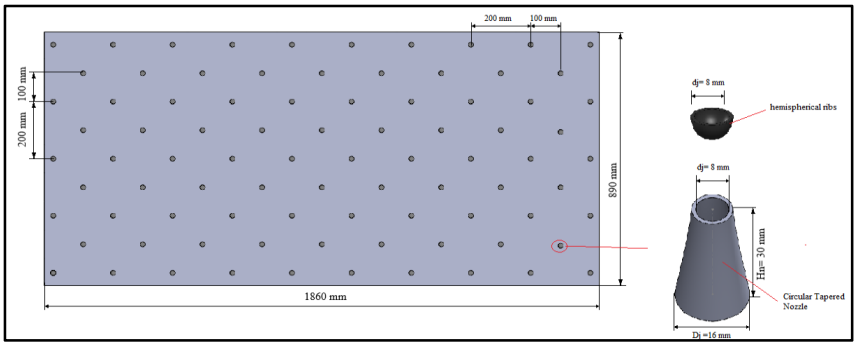

Fig. 2 Isometric view of the hemispherical ribs and circular tapered nozzle

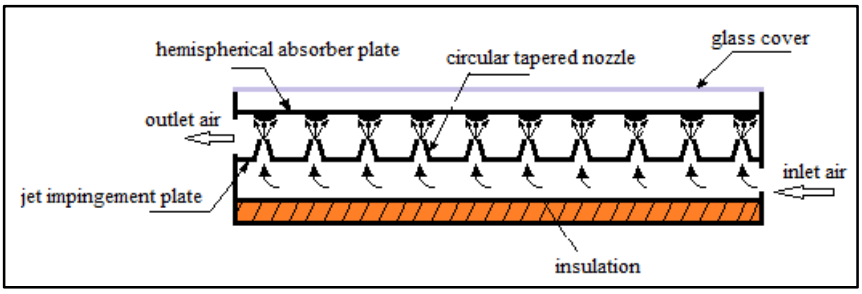

Fig. 3 Schematic view of HAP-CTN-JIPSAC

Table 1. Properties of HAP-CTN-JIPSAC and CFD domains.

Part	Material	Dimension (mm)	Thermal Properties
collector case	double wall galvanized sheet insulated with elastomeric rubber foam	1860x890x400	ε: 0.7, λ:2.11x10^{-5} W/cm-K
glass cover	glass	1860x890x2	ε: 0.92, λ:0.0078 W/cm-K, C_p: 0.84 J/g K
hemispherical absorber plate	matt black painted sheet	1860x890x0.6	ε: 0.9, λ:52 W/m-K, C_p: 0.470 J/g K
jet impinging plate	galvanized sheet	1860x890x1	ε: 0.54, λ:0.52 W/cm-K, C_p: 0.47 J/g K
intermediate sheet	galvanized sheet with one surface insulated with elastomeric rubber foam	1860x890x0.6	ε: 0.7, λ:2.11x10^{-5} W/cm-K, C_p: 0.84 J/g K
bottom insulation	glass wool	1860x890x186	λ:38x10^{-5} W/cm-K, ρ:0.024 g/cm^3, C_p: 0.7 J/g K
air	atmospheric air		ε: 0.3, λ :25,63x10^{-5} W/cm-K, ρ:0.00120 g/cm^3 , Cp: 1.004 J/g K

2.3. Meshing of HAP-CTN-JIPSACs fluent volume

Simulations to obtain accurate results in CFD analysis it depends on the correct size and regular distribution of finite elements in the network. In the current mesh formation, the best mesh was formed with a average skewnes of 0.25017 and aspect ratio of 1.8774 with a total number of 3779062 elements. The meshing of the current design of HAP-CTN-JIPSAC can be seen in fig. 4. In network improvement studies, the difference between two consecutive results is less than 1%.

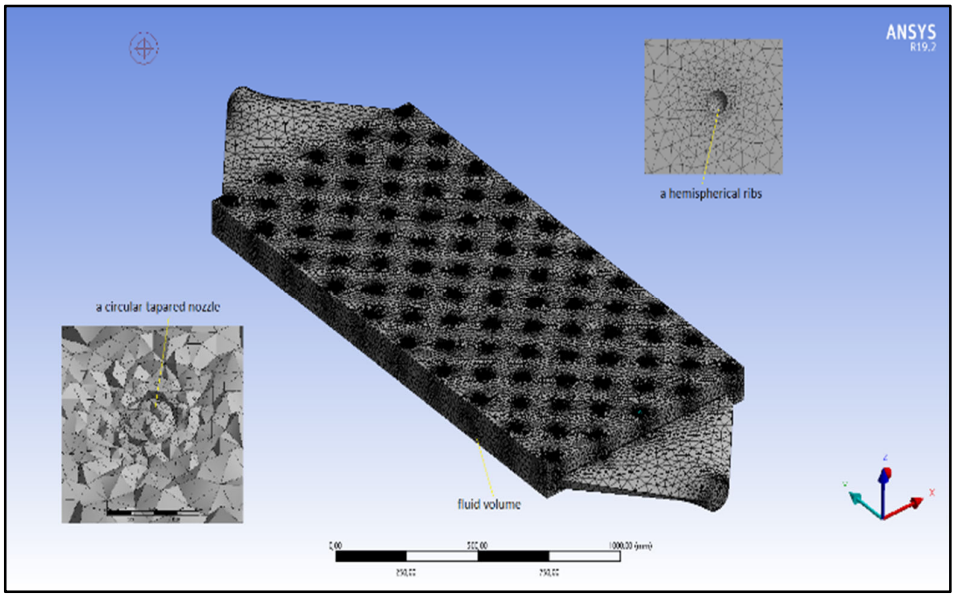

Fig. 4. The meshing of the current design of HAP-CTN-JIPSAC

2.4. Governing equations and applied boundary conditions and solution method

In this study, the flow form was accepted as incompressible turbulent flow because the speed range was <0.3 Mach and the density change depending on speed was less than 5% [85]

The 3D continuity equation, Navier-Stokes and energy equation solved in Ansys Fluent are given in eq.(1-3).

Continuity equation;

$$\frac{\partial(\rho u_i)}{\partial x_i} = 0 \tag{1}$$

Navier-stokes equation;

$$\frac{\partial}{\partial x_i}(\rho u_i u_j) = -\frac{\partial p}{\partial x_i} + \frac{\partial}{\partial x_j}\left[\mu\left(\frac{\partial(\rho u_i)}{\partial x_i} + \frac{\partial(\rho u_i)}{\partial x_i}\right)\right] + \frac{\partial}{\partial x_j}\left(-\overline{\rho u_i u_j}\right) \tag{2}$$

Energy conservation equation;

$$\frac{\partial}{\partial x_i}(\rho u_i T) = \frac{\partial}{\partial x_j}\left[\left(\frac{\mu}{Pr} + \frac{\mu}{Pr_t}\right)\right]\left(\frac{\partial T}{\partial x_j}\right) \tag{3}$$

The convection, pressure gradient, and viscous factors, respectively, in all three directions are represented by the first, second, and third terms in eq. (2). [86]. This study was carried out at boundary conditions of in flow 0.0046, 0.0092, 0.0139 and 0.0185 kg/s (1, 2, 3 and 4 m/s air inlet velocities), respectively, and at an outdoor air inlet temperature of 17.7 ºC in parallel with the experimental study. The simulation was run with the Rosseland radiation model at 38.21854 longitude and 37.74748 latitude.

The physics of flow and boundary conditions applied in CFD simulation determine the choice of solver model.

Model selection depends upon the physics of flow and boundary conditions used in CFD simulation. Accordingly, the governing equations in this study are solved using the pressure-based solver and the finite volume approach in the steady-state domain.

3. Experımental Setup

3.1. performance parameters of HAP-CTN-JIPSAC.

The thermal efficiency of the HAP- CTN-JIPSAC was computed with eq. (4-5).

The useful heat gain of air is calculated as [87]:

$$Qu = \dot{m}.Cp.(T_o - T_i) \quad (4)$$

where, ṁ is the mass flow rate of air (kg/s), C_p specific heat property of air at constant pressure (kJ/kg. K), T_i and T_o are the inlet and outlet air temperatures respectively. The heat transfer coefficient of solar aircollector was computed with eq. (5) [92].

$$h = \frac{Q_u}{A_a\,(T_p - T_a)} \quad (5)$$

Where; T_p and T_a are the mean plate and working air temperatures, respectively, and A_a is the absorber surface area.

3.2. Description of the experimental setup

A schematic representation of the experimental apparatus used in this work is shown in fig. 5. The photographic view of the circular tapared nozzle and hemispherical absorber plate used in the experimental study is shown in fig.6-7. The properties of the SAC with hemispherical absorber plate and circular tapered nozzle pair (HAP- CTN-JIPSAC) used in the experimental study are given in Table 1. To guarantee that the input air is distributed evenly and to gather and move the heated air to the consumption area, two hoods are installed case- material.

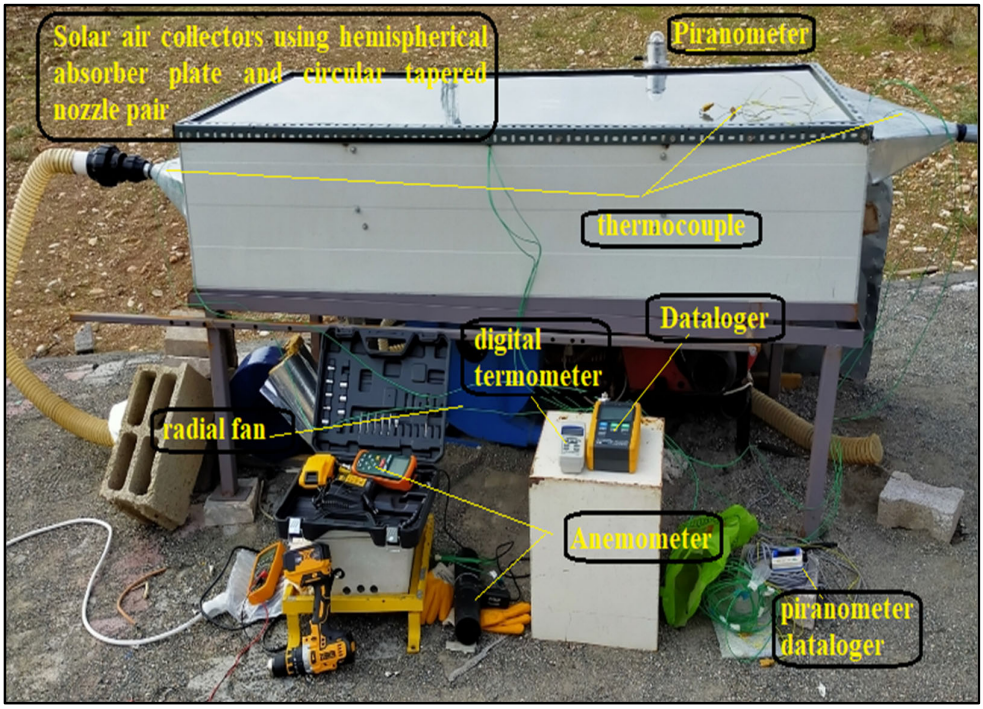

Fig. 5. Image of the HAP-CTN-JIPSAC experimental setup

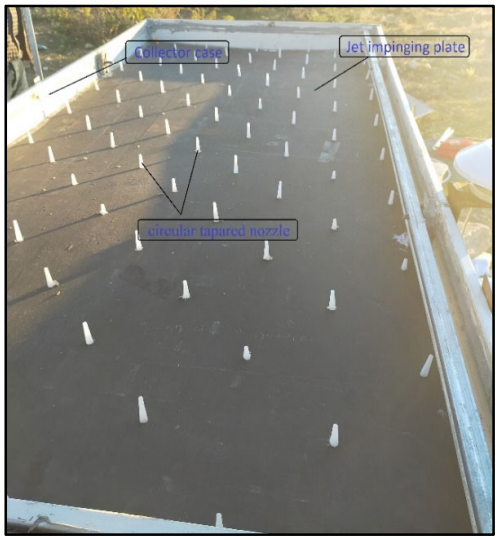

Fig. 6. Image of the jet impinging plate with circular tapared nozzle

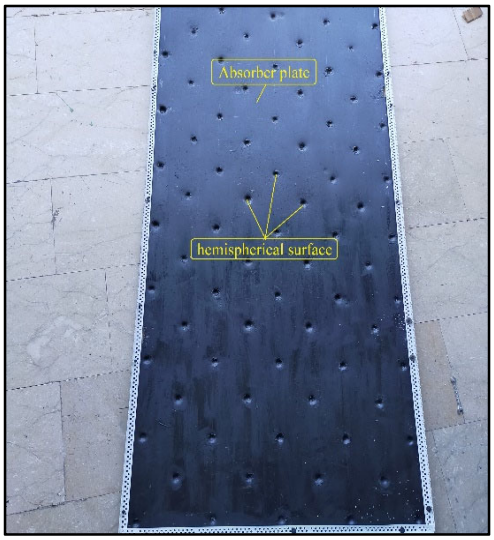

Fig. 7. Image of the the hemispherical absorber plate

3.3. Error Analysis

An error analysis was carried out to assess the accuracy of the model and the anticipated outcomes for the air temperature at various HAP- CTN-JIPSAC locations, air inlet velocity and were compared with the corresponding experimental data. The Holman JP technique is used to determine the percentage of absolute error values [88].

$$U_F = \left[\left(\frac{\partial F}{\partial z_1} u_1\right)^2 + \left(\frac{\partial F}{\partial z_2} u_2\right)^2 + \ldots + \left(\frac{\partial F}{\partial z_n} u_n\right)^2\right]^{1/2} \quad (6)$$

In table 2. is presented full breakdown of the uncertainty values resulting from the measurement of several parameters during the current experimental examination.

Table 2. Total uncertainties of HAP- CTN-JIPSAC

The evaluation of the uncertainty in CTN-JIPSAC	Symbol	Unit	Accuracy	Total uncertainty (%)
Collector inlet air temperature	T_o	°C	±0.5	0.287
Collector outlet air temperature	T_i	°C	±0.1	0.424
Collector inlet air velocity	v	m/s	±0.01	0.104
Solar radiation	I	W/m^2	±0.03	0.0316
Calculated parameters				
Mass flow rate of air	ṁ	kg/s		0.06
Thermal efficiency of collector	η	%		0.202

4. Experimental Analysis of HAP- CTN-JIPSAC

Inlet and outlet temperature variation with solar radiation at different air flow rates for HAP-CTN-JIPSAC is given in Fig.8 and collector efficiency at different flow rates is given in Fig.9. It has been observed that as solar radiation increases, the collector exit temperature increases and a significant

temperature difference occurs between the collector inlet and outlet. It is seen in the figures that the difference between the average T_i and T_o varies between 8.02-34,38 ºC depending on solar radiation. It has been also observed that transfers the energy stored in the collector's absorber plate to the working air when the sun is clouded for a short time and ensures continuity in collector efficiency during these moments.

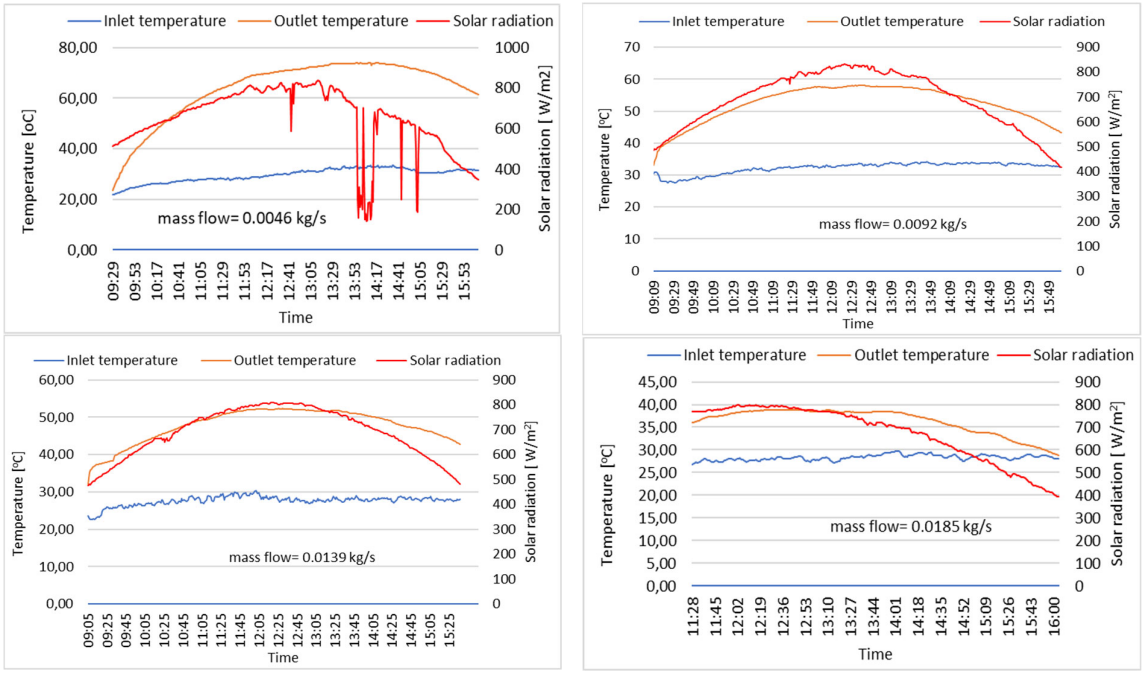

Fig. 8. Inlet and outlet temperature variation by solar radiation at different flow rates

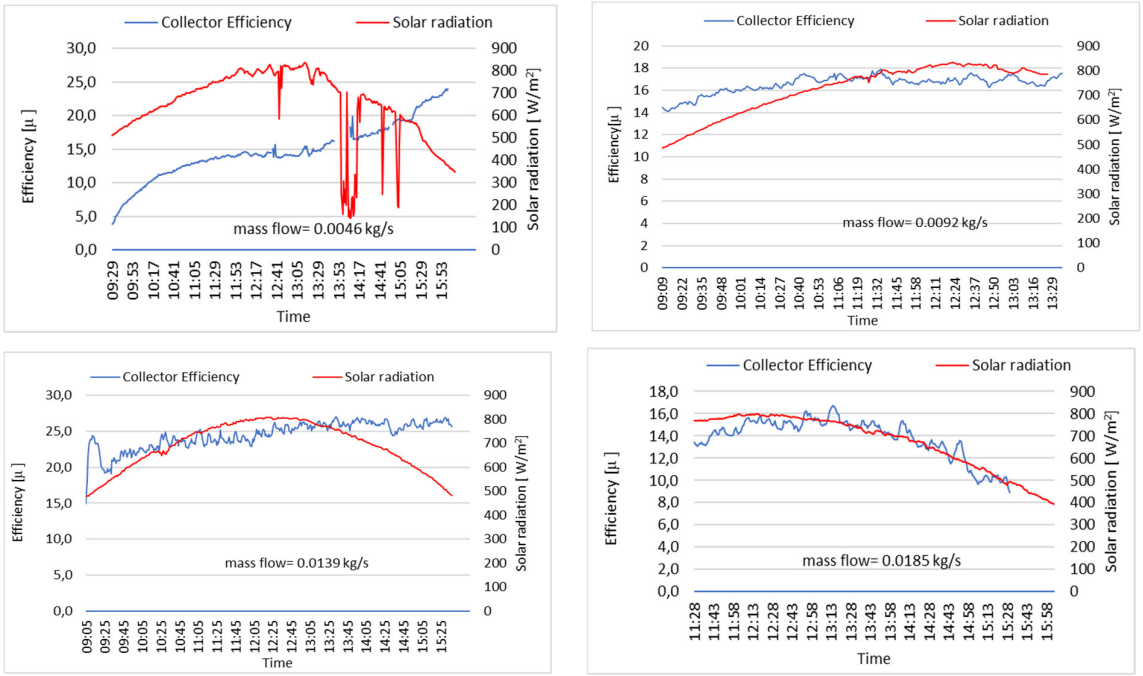

Fig. 9. Collector efficiency at different flow rates

In experimental previus studies on FPSAC, higher outlet temperatures have been noted at low flow rates, and as flow rates rise, outlet temperatures have been shown to drop. Although the difference between the maximum outlet temperature (To max.) and the minimum outlet temperature (To min.) ΔTo= 29.8 ºC at FPSAC, it was seen to ΔTo = 37,3 ºC in JIPSAC. With the use of the hemispherical absorber plate (HAP- CTN-JIPSAC), this difference increased up to 41.9 ºC.

In HAP- CTN-JIPSAC, it has been observed that the average highest efficiency of the collector was observed as ηav.=24.5%, To av.=47.8 ºC when ṁ=0.0139 kg/s. Variation of collector minimum, average and maximum efficiency with mass flow rate is given in Fig.10.

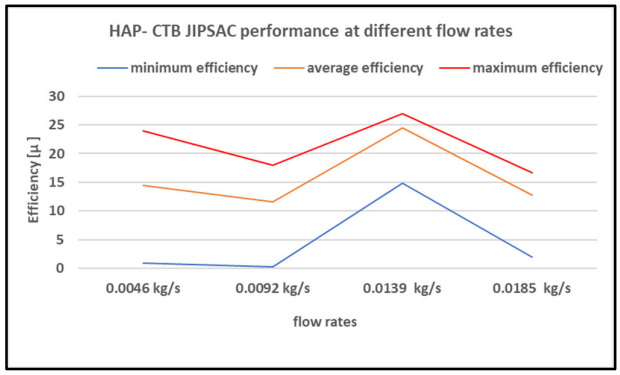

Fig 10. Variation of collector minimum, average and maximum efficiency with mass flow rate

5. Numerical Analysis of HAP- CTN-JIPSAC

This section provides a detailed discussion of the findings from the CFD analysis of the current HAP-CTN-JIPSAC design. The jet impinging region's contours of temperature, pressure, and velocity are represented by the thermo-hydraulic performance enhancement.

In order to compare the experimental studies carried out to investigate the effect of solar radiation on the collector outlet temperature and thermal efficiency in Adıyaman/Turkey climatic conditions, at 17.7 ºC air inlet temperature and of in flow 0.0046, 0.0092, 0.0139 and 0.0185 kg/s (1, 2, 3 and 4 m/s air inlet velocities), CFD analyzes were performed. The inlet air temperature was taken as 17.7 °C in order to provide the same boundary conditions as the CFD analysis results in the experimental study conducted at a flow rate of 0.0046 kg/s. The data obtained from the simulation largely confirm the measurements obtained from the experimental study. In other numerical analyses, since the inlet temperature changes depending on daily solar radiation and outside air temperature, only the flow rate is changed by keeping the inlet air temperature constant. The calculation results are in agreement with the experimental values of collector outlet temperatures with a margin of error of ± 3%.

The temperature distributions and velocity contours of HAP- CTN-JIPSAC are given in fig. 11-12. From the simulation results, it was revealed that the mass flow rate was 0.0139 kg/s and occurred at a linear speed. CFD analyses showed volumes where the air distribution inside the duct was not balanced due to the design geometry. In cases where the flow rate is lower, it has been observed that ineffective volumes are formed in the lower channel near the inlet of the collector internal volume. Since the speed was insufficient, no flow occurred in the jet nozzles close to the exit. It has been observed that when the flow rate is greater than 0.0139 kg/s, the pressure losses increase and the time for the air to gain energy decreases, thus the outlet temperature is low and the collector efficiency decreases.

Fig. 13 show the pressure contours in the HAP- CTN-JIPSAC at different flow rates. The formation of the flow volume is given in Fig. 14 volume formation varies depending on the flow rate at the collector inlet. It is evident that as air velocity gradually decreases approaching the exit, the pressure drop grows significantly larger in a longitudinal direction. Furthermore, when the air flow rate increases,

so does the pressure loss. Bunun nedeni, çapraz akış durumlarının ve jet akışı girişimlerinin daha yüksek pompalama ihtiyacına yol açan sürtünme kayıpları oluşturmasıdır.

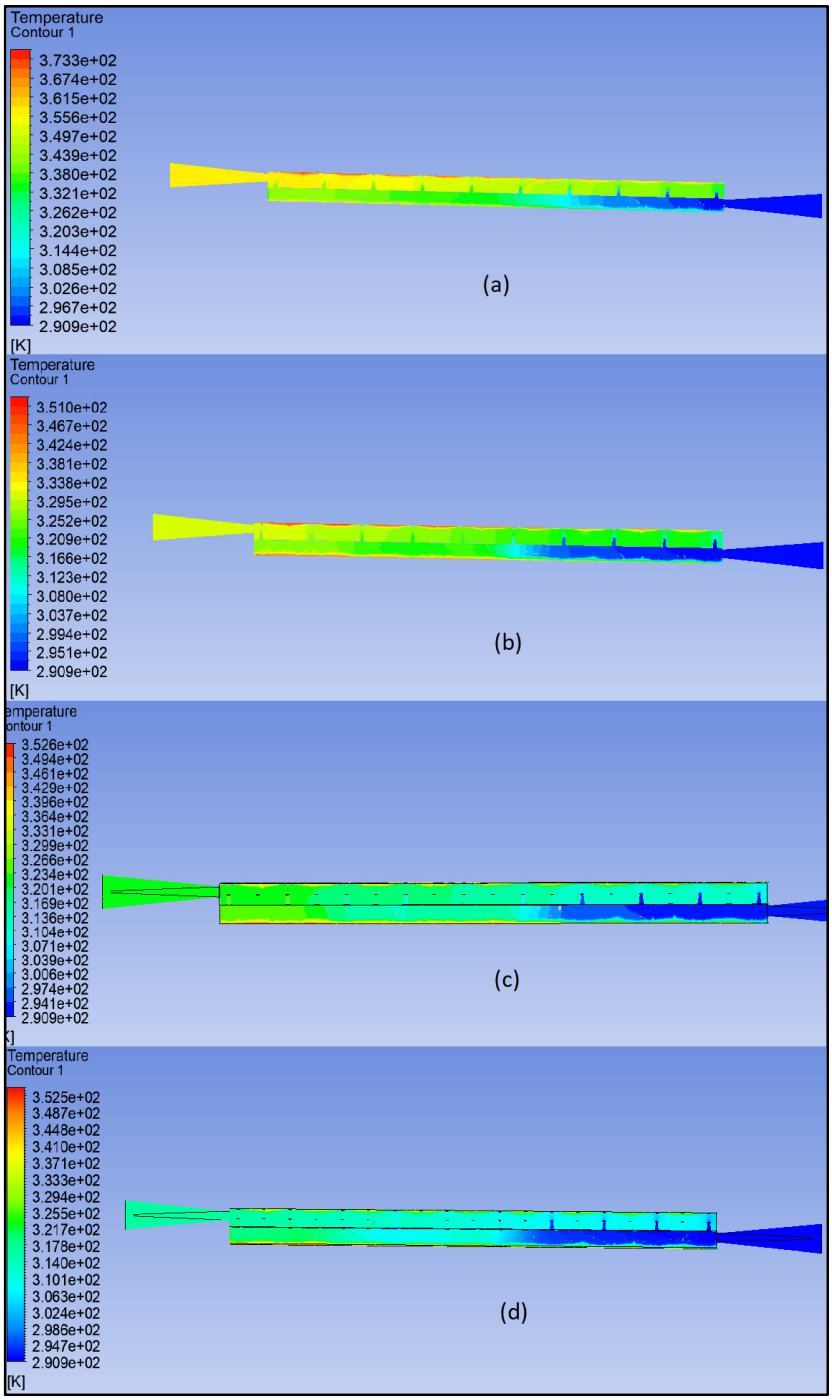

Fig. 11. Temperature contours of HAP- CTN-JIPSAC for in flow at (a) 0.0046 (b) 0.0092, (c)0.0139 and (d)0.0185 kg/s

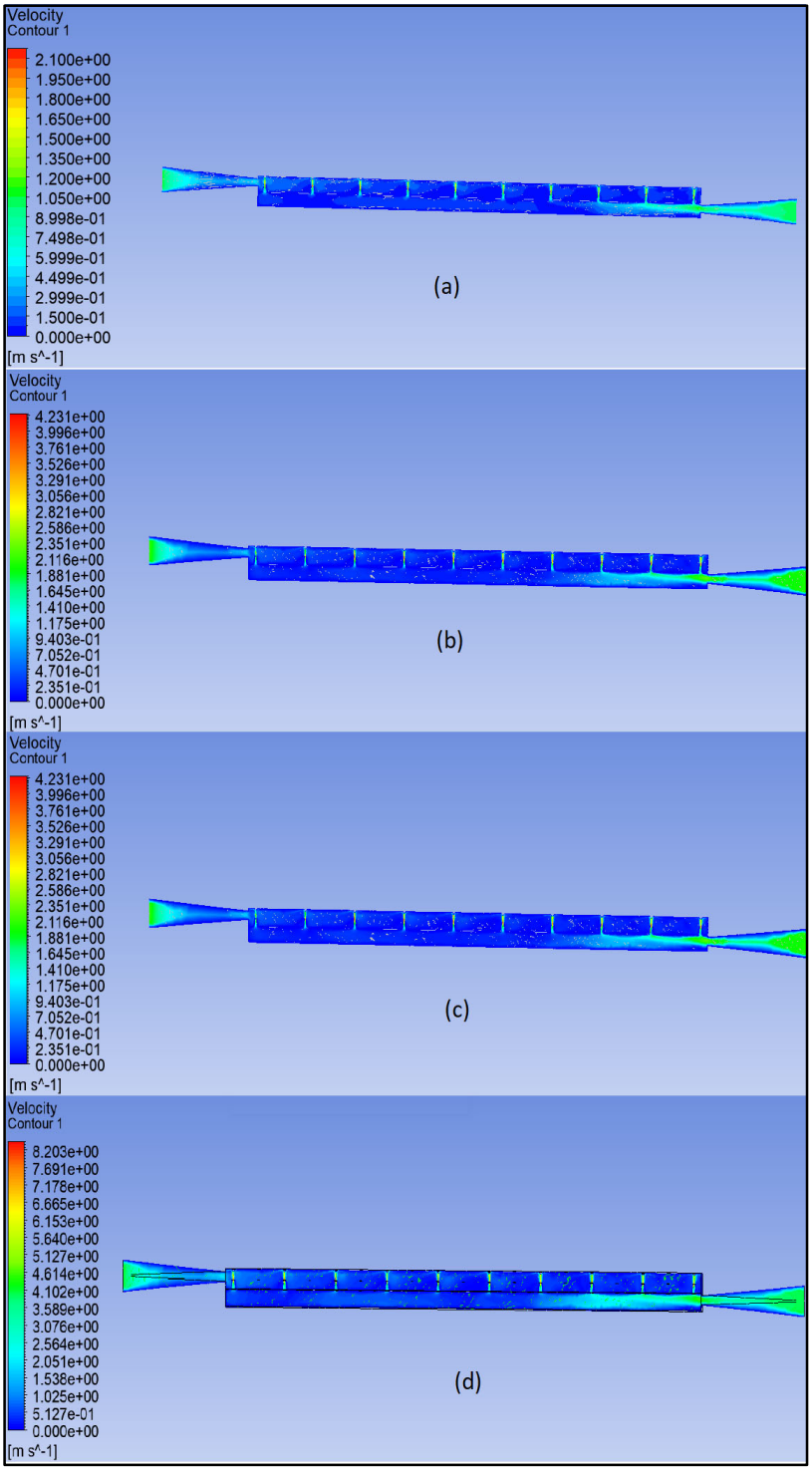

Fig. 12. Velocity contours of HAP- CTN-JIPSAC for in flow at (a) 0.0046 (b) 0.0092, (c)0.0139 and (d)0.0185 kg/s

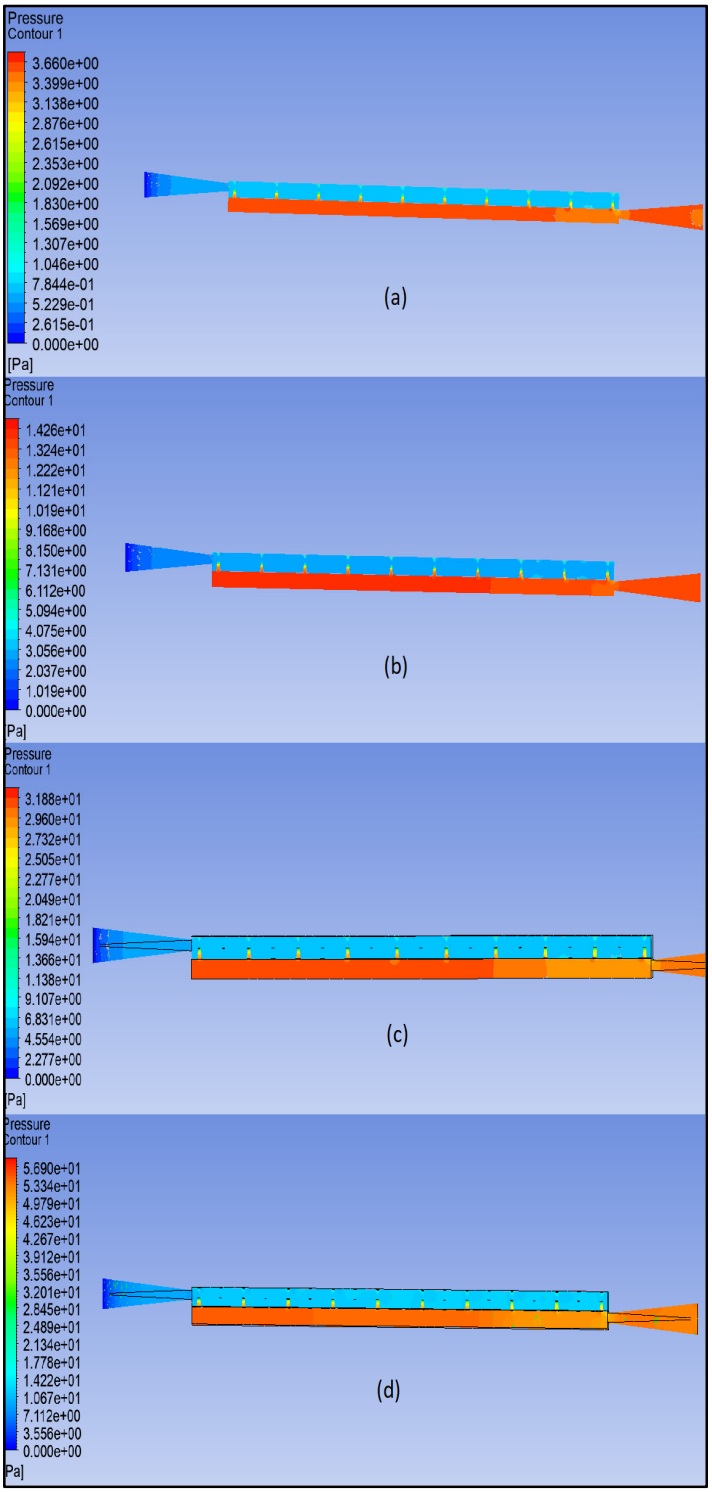

Fig. 13. Pressure contours of HAP- CTN-JIPSAC for in flow at (a) 0.0046 (b) 0.0092, (c)0.0139 and (d)0.0185 kg/s

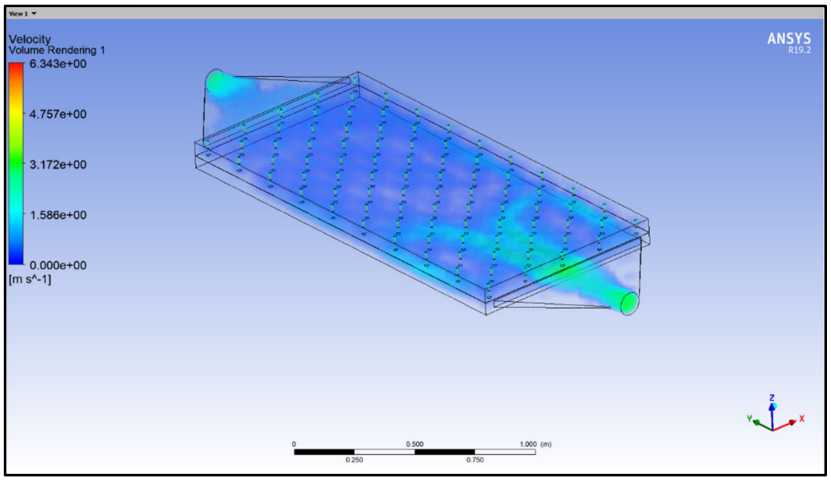

Fig. 14. Volume rendering of HAP- CTN-JIPSAC

6. Conclusions and Recommendations

The purpose of the experimental study was to investigate the impact of hemıspherıcal absorber plate on the collector efficiency used in the HAP- CTN- JIPSAC at mass flow rates of 0.0046, 0.0092, 0.0139, and 0.0185 kg/s (air inlet velocities of 1, 2, 3, and 4 m/s). According to the measured data, the highest air outlet temperature was measured at 73.9 ºC at low flow rate $\dot{m}$ = 0.0046 kg/s. In experimental and numerical analyzes on the HAP- CTN- JIPSAC it was noted that when there was less air flow, the collector outlet temperature was higher. on the contrary as the flow rate increased, a reduction in exit temperature was noted. The best average collector outlet temperature was measured as 63.9 ºC when the mass flow rate is 0.0046 kg/s. The best average thermal efficiency in the collector was calculated as 24.5 % when the mass flow rate is 0.0139 kg/s.

When the flow rate is low, the outlet temperature is higher because enough time has passed for the fluid air to heat up sufficiently. However, when the flow rate increases, the collector efficiency increases as there is more useful energy gain. At very high flow rates, the outlet temperature decreases because there is less time for the air to receive enough energy.

The results of the CFD analysis showed that as the collector size increases and the jet effect in the outlet direction decreases and that the jet flow coming out of the conical nozzle on the absorber plate should be slow and regular over the rib surface area for higher thermal efficiency

More industrial models should be developed and more powerful fans should be used for experimental studies with different configurations and flow rates. In addition, the compatibility of the jet nozzle geometry and the absorber plate rib geometry should be improved.

Acknowledgements

This study was supported by Harran University Scientific Research Project Unit within the scope of project no. 19249.

Conflict Of Interest

The authors declare that they have no conflict of interest

Reference

[1] Sureandhar, G., Srinivasan, G., Muthukumar, P., Senthilmurugan, S., 2021. Performance analysis of arc rib fin embedded in a solar air heater. Therm. Sci. Eng. Prog. 23 https://doi.org/10.1016/j.tsep.2021.100891.

[2] Rahmani, E., Moradi, T., Fattahi, A., Delpisheh, M., Karimi, N., Ommi, F., et al., 2021. Numerical simulation of a solar air heater equipped with wavy and raccoon-shaped f ins: The effect of fins' height. Sustain Energy Technol. Assess. 45, 101227 https:// doi.org/10.1016/j.seta.2021.101227.

[3] Parsa, H., Saffar-Avval, M., Hajmohammadi, M.R., 2021. 3D simulation and parametric optimization of a solar air heater with a novel staggered cuboid baffles. Int J. Mech. Sci. 205, 106607 https://doi.org/10.1016/j.ijmecsci.2021.106607.

[4] Amara, W.B., Bouabidi, A., 2023. Experimental studies and 3D simulations for the investigation of thermal performances of a solar air heater with different spiral- shaped baffles heights. J. Build. Eng. 65, 105662.

[5] Khanlari, A., Tuncer, A.D., S¨ ozen, A., Aytaç, ˙ I., Çiftçi, E., Variyenli, H.˙ I., 2022. Energy and exergy analysis of a vertical solar air heater with nano-enhanced absorber coating and perforated baffles. Renew. Energy 187, 586–602.

[6] Selimefendigil, F., S ¸irin, C., Ghachem, K., Kolsi, L., Alqahtani, T., Algarni, S., 2022b. Enhancing the performance of a greenhouse drying system by using triple-flow solar air collector with nano-enhanced absorber coating. Case Stud. Therm. Eng. 34, 102011.

[7] Oztürk, M., Yüksel, C., Çiftçi, E., 2024. Investigation of a Photovoltaic–Thermal Solar Dryer System with Double-Pass Solar Air Collectors and Absorber Surfaces Enhanced with Graphene Nanoparticles. Arab. J. Sci. Eng. https://doi.org/10.1007/s13369- 024-08717-z.

[8] Jasyal, N.K., Sharma, S.L., Debbarma, A., 2023. Performance analysis of solar air heater using triangular corrugated absorber under jet impingement. Energy Sources, Part A: Recovery, Util., Environ. Eff. 45 (3), 9063–9080.

[9] Ho, C.D., Lin, C.S., Chuang, Y.C., Chao, C.C., 2013. Performance improvement of wire mesh packed double-pass solar air heaters with external recycle. Renew. Energy 57, 479–489.

[10] Gürbüz, E.Y., Sahinkesen, ˙ I., Kusun, B., Tuncer, A.D., Keçebas¸, A., 2023. Enhancing the performance of an unglazed solar air collector using mesh tubes and Fe3O4 nano- enhanced absorber coating. Energy 277, 127704.

[11] Dong, Z., Du, Q., Liu, P., Liu, Z., Liu, W., 2023. A numerical investigation and irreversibility optimization of constantly grooved solar air heaters. Renew. Energy 207, 629–646.

[12] Tuncer, A.D., Amini, A., Khanlari, A., 2023. Developing an infrared-assisted solar drying system using a vertical solar air heater with perforated baffles and nano-enhanced black paint. Sol. Energy 263, 111958.

[13] Alomar, O.R., Abd, H.M., Salih, M.M.M., 2022. Efficiency enhancement of solar air heater collector by modifying jet impingement with v-corrugated absorber plate. J. Energy Storage 55, 105535.

[14] Farzan, H., Hasan Zaim, E., 2023. Study on thermal performance of a new combined perforated Metallic/Asphalt solar air heater for heating Applications: An experimental study. Sol. Energy 249, 485–494. https://doi.org/10.1016/j. solener.2022.12.008.

[15] W. Gao, W. Lin, T. Liu, and C. Xia, "Analytical and experimental studies on the thermal performance of cross-corrugated and flat-plate solar air heaters," Appl. Energy, vol. 84, no. 4, pp. 425–441, 2007, doi: https://doi.org/10.1016/j.apenergy.2006.02.005.

[16] T. A. Yassen, N. D. Mokhlif, and M. Asmail, "Performance investigation of an integrated solar water heater with corrugated absorber surface for domestic use," Renew. Energy, vol. 138, pp. 852–860, 2019, doi: 10.1016/j.renene.2019.01.114.

[17] S.A. Abdel-Moneim Atwan, E.F. Atwan, and A.R. El-Shamy, "Heat Transfer and Flow Friction in a Rectangular Duct with Repeated Multiple v-ribs Mounted on the Bottom Wall," in 12th International Mechanical Power Engineering Conference (IMPEC12), 2001, pp. 11–25.

[18] C.-O. Olsson and B. Sunden, "Thermal and Hydraulic Performance of a Rectangular Duct With Multiple V-Shaped Ribs," J. Heat Transfer, vol. 120, no. 4, pp. 1072–1077, Nov. 1998, doi: 10.1115/1.2825892.

[19] J. C. Han, Y. M. Zhang, and C. P. Lee, "Augmented Heat Transfer in Square Channels With Parallel, Crossed, and V-Shaped Angled Ribs," J. Heat Transfer, vol. 113, no. 3, pp. 590–596, Aug. 1991, doi: 10.1115/1.2910606.

[20] E. A. M. Elshafei, M. M. Awad, E. El-Negiry, and A. G. Ali, "Heat transfer and pressure drop in corrugated channels," Energy, vol. 35, no. 1, pp. 101–110, Jan. 2010, doi: 10.1016/J.ENERGY.2009.08.031.

[21] H. Pehlivan, I. Taymaz, and Y. İ, "Experimental study of forced convective heat transfer in a different arranged corrugated channel," Int. Commun. Heat Mass Transf., vol. 46, pp. 106–111, 2013, doi: 10.1016/j.icheatmasstransfer.2013.05.016.

[22] M. A. Mehrabian and R. Poulter, "Hydrodynamics and thermal characteristics of corrugated channels: computational approach," Appl. Math. Model., vol. 24, no. 5, pp. 343–364, 2000, doi: https://doi.org/10.1016/S0307-904X(99)00039-6.

[23] K. Sarraf, S. Launay, and L. Tadrist, "Complex 3D-flow analysis and corrugation angle effect in plate heat exchangers," Int. J. Therm. Sci., vol. 94, pp. 126–138, 2015, doi: https://doi.org/10.1016/j.ijthermalsci.2015.03.002.

[24] Y. Qin, X. Guan, Z. Dun, and H. Liu, "Numerical simulation on fluid flow and heat transfer in a corrugated plate air preheater," Dongli Gongcheng Xuebao/Journal Chinese Soc. Power Eng., vol. 35, pp. 213–218, Mar. 2015.

[25] C. Zimmerer, P. Gschwind, G. Gaiser, and V. Kottke, "Comparison of heat and mass transfer in different heat exchanger geometries with corrugated walls," Exp. Therm. Fluid Sci., vol. 26, no. 2, pp. 269–273, 2002, doi: https://doi.org/10.1016/S0894-1777(02)00136-X.

[26] J. E. O'Brien and E. M. Sparrow, "Corrugated-Duct Heat Transfer, Pressure Drop, and Flow Visualization," J. Heat Transfer, vol. 104, no. 3, p. 410, Aug. 1982, doi: 10.1115/1.3245108.

[27] Y. Islamoglu and C. Parmaksizoglu, "The effect of channel height on the enhanced heat transfer characteristics in a corrugated heat exchanger channel," Appl. Therm. Eng., vol. 23, no. 8, pp. 979–987, Jun. 2003, doi: 10.1016/S1359-4311(03)00029-2.

[28] A. Hamza, H. Ali, and Y. Hanaoka, "Experimental study on laminar flow forced-convection in a channel with upper V-corrugated plate heated by radiation," Int. J. Heat Mass Transf., vol. 45, no. 10, pp. 2107–2117, 2002.

[29] Salman, M., Chauhan, R., Poongavanam, G. K., & Kim, S. C., 2022. Analytical investigation of jet impingement solar air heater with dimple-roughened absorber surface via thermal and effective analysis. Renewable Energy, 199, 1248-1257.

[30] Zhu, T. T., Diao, Y. H., Zhao, Y. H., & Deng, Y. C., 2015. Experimental study on the thermal performance and pressure drop of a solar air collector based on flat micro-heat pipe arrays. Energy conversion and management, 94, 447-457.

[31] R. Chauhan and N. S. Thakur, "Heat transfer and friction factor correlations for impinging jet solar air heater," Exp. Therm. Fluid Sci., vol. 44, pp. 760–767, 2013, doi: 10.1016/j.expthermflusci.2012.09.019.

[32] M. A. R. Sharif and A. Banerjee, "Numerical analysis of heat transfer due to confined slot-jet impingement on a moving plate," Appl. Therm. Eng., vol. 29, no. 2–3, pp. 532–540, Feb. 2009, doi: 10.1016/J.APPL THERMA LENG. 2008.03.011.

[33] M. Imbriale, A. Ianiro, C. Meola, and G. Cardone, "Convective heat transfer by a row of jets impinging on a concave surface," Int. J. Therm. Sci., vol. 75, pp. 153–163, Jan. 2014, doi: 10.1016/J.IJTHERMALSCI.2013.07.017.

[34] E. Öztekin, O. Aydin, and M. Avcı, "Heat transfer in a turbulent slot jet flow impinging on concave surfaces," Int. Commun. Heat Mass Transf., vol. 44, pp. 77–82, May 2013, doi: 10.1016/J.ICHEATMASSTRANSFER.2013.03.006.

[35] M. Kilic, T. Calisir, and S. Baskaya, "Experimental and numerical study of heat transfer from a heated flat plate in a rectangular channel with an impinging air jet," J. Brazilian Soc. Mech. Sci. Eng., vol. 39, no. 1, pp. 329–344, 2017, doi: 10.1007/s40430-016-0521-y.

[36] N. Celik and E. Turgut, "Design analysis of an experimental jet impingement study by using Taguchi method," Heat Mass Transf., vol. 48, no. 8, pp. 1407–1413, 2012, doi: 10.1007/s00231-012-0989-7.
[37] A. J. Onstad, T. B. Hoberg, C. J. Elkins, J. K. Eaton, and E. Mall, "Sixth International Symposium on Turbulence and Shear Flow Phenomena flow and heat transfer for jet impingement arrays with local extraction," no. June, pp. 22–24, 2009.
[38] R. Chauhan and S. C. Kim, "Effective efficiency distribution characteristics in protruded/dimpled-arc plate solar thermal collector," Renew. Energy, vol. 138, pp. 955–963, 2019, doi: https://doi.org/10.1016/j.renene.2019.02.050.
[39] G. Yang, M. Choi, and J. S. Lee, "An experimental study of slot jet impingement cooling on concave surface: Effects of nozzle configuration and curvature," Int. J. Heat Mass Transf., vol. 42, no. 12, pp. 2199–2209, 1999, doi: 10.1016/S0017-9310(98)00337-8.
[40] P. Culun, N. Celik, and K. Pihtili, "Effects of design parameters on a multi jet impinging heat transfer," Alexandria Eng. J., vol. 57, no. 4, pp. 4255–4266, 2018, doi: https://doi.org/10.1016/j.aej.2018.01.022.
[41] A. M. Aboghrara et al., "Parametric study on the thermal performance and optimal design elements of solar air heater enhanced with jet impingement on a corrugated absorber plate," Int. J. Photoenergy, vol. 2018, 2018, doi: 10.1155/2018/1469385.
[42] M. Belusko, W. Saman, and F. Bruno, "Performance of jet impingement in unglazed air collectors," vol. 82, pp. 389–398, 2008, doi: 10.1016/j.solener.2007.10.005.
[43] R. Ekiciler, M. S. A. Çetinkaya, and K. Arslan, "Convective Heat Transfer Investigation of a Confined Air Slot-Jet Impingement Cooling on Corrugated Surfaces With Different Wave Shapes," J. Heat Transfer, vol. 141, no. 2, p. 022202, 2018, doi: 10.1115/1.4041954.
[44] N. K. Chougule, G. V Parishwad, and C. M. Sewatkar, "Numerical Analysis of Pin Fin Heat Sink with a Single and Multi Air Jet Impingement Condition," vol. 1, no. 3, pp. 44–50, 2012
[45] A. kumar Goel, S. N. Singh, and B. N. Prasad, "Experimental investigation of thermo-hydraulic efficiency and performance characteristics of an impinging jet-finned type solar air heater," Sustain. Energy Technol. Assessments, vol. 52, Aug. 2022.
[46] R.K. Nayak, S.N. Singh, Effect of geometrical aspects on the performance of jet plate solar air heater, Sol. Energy. 137 (2016) 434–440, https://doi.org/10.1016/j. solener.2016.08.024.
[47] Kercher DM, Tabakoff W, Heat Transfer by a square array of round air jets impinging perpendicular to a flat surface including the effect of spent air, ASME- Paper 69-GT-4. (1969). https://asmedigitalcollection.asme.org/gasturbinespower
[48] J.E. Ferrari, N. Lior, J. Slycke, An evaluation of gas quenching of steel rings by multiple-jet impingement, J. Mater. Process. Technol. 136 (2003) 190–201, https://doi.org/10.1016/S0924-0136(03)00158-4.
[49] L.W. Florschuetz, C.R. Truman, D.E. Metzger, Streamwise flow and heat transfer distributions for jet array impingement with crossflow., Am. Soc. Mech. Eng. (1981) 1–10. http://proceedings.asmedigitalcollection.asme.org/.
[50] L.F.G. Geers, M.J. Tummers, T.J. Bueninck, K. Hanjali´ c, Heat transfer correlation for hexagonal and in-line arrays of impinging jets, Int. J. Heat Mass Transf. 51 (2008) 5389–5399, https://doi.org/10.1016/j.ijheatmasstransfer.2008.01.035.
[51] M. Goodro, J. Park, P. Ligrani, M. Fox, H.K. Moon, Effects of hole spacing on spatially-resolved jet array impingement heat transfer, Int. J. Heat Mass Transf. 51 (2008) 6243–6253, https://doi.org/10.1016/j.ijheatmasstransfer.2008.05.004.
[52] J. Lee, Z. Ren, P. Ligrani, D.H. Lee, M.D. Fox, H.K. Moon, Cross-flow effects on impingement array heat transfer with varying jet-to-target plate distance and hole spacing, Int. J. Heat Mass Transf. 75 (2014) 534–544, https://doi.org/10.1016/j. ijheatmasstransfer.2014.03.040.
[53] C. Choudhury, H.P. Garg, Evaluation of a jet plate solar air heater, Sol. Energy. 46 (1991) 199–209, https://doi.org/10.1016/0038-092X(91)90064-4.
[54] Metzger, D. E., Florschuetz, L. W., Takeuchi, D. I., Behee, R. D., & Berry, R. A., 1979. Heat transfer characteristics for inline and staggered arrays of circular jets with crossflow of spent air. ASME Journal of Heat Transfer, 101 (3), 526–531 https://doi.org/10.1115/1.3451022.

[55] R. Moshery, T.Y. Chai, K. Sopian, A. Fudholi, A.H.A. Al-Waeli, Thermal performance of jet-impingement solar air heater with transverse ribs absorber plate, Sol. Energy. 214 (2021) 355–366, https://doi.org/10.1016/j. solener.2020.11.059.
[56] Song, Z., Xue, Y., Jia, B., He, Y., 2023. Introduction of the rectangular hole plate in favor the performance of photovoltaic thermal solar air heaters with baffles. Appl. Therm. Eng. 220, 119774.
[57] Tan, A.S.T., Janaun, J., Tham, H.J., Siambun, N.J., Abdullah, A., 2022. Performance analysis of a solar heat collector through experimental and CFD investigation. Mater. Today.: Proc. 57, 1338–1344.
[58] S. Kumar et al., "CFD analysis of the influence of distinct thermal enhancement techniques on the efficiency of double pass solar air heater (DP-SAH)," Materials Today: Proceedings, Jun. 2023, doi: 10.1016/j.matpr.2023.05.454.
[59] Arya, N., Goel, V., Sunden, B., 2023. Solar air heater performance enhancement with differently shaped miniature combined with dimple shaped roughness: CFD and experimental analysis. Sol. Energy 250, 33–50.
[60] Potgieter, M.S.W., Bester, C.R., Bhamjee, M., 2020. Experimental and CFD investigation of a hybrid solar air heater. Sol. Energy 195, 413–428.
[61] Tuncer, A.D., Khanlari, A., S¨ ozen, A., Gürbüz, E.Y., S¸irin, C., Gungor, A., 2020. Energy- exergy and enviro-economic survey of solar air heaters with various air channel modifications. Renew. Energy 160, 67–85.
[62] Kumar, S., & Saini, R. P., 2009. CFD based performance analysis of a solar air heater duct provided with artificial roughness. Renewable energy, 34(5), 1285-1291.
[63] Karmare, S. V., & Tikekar, A. N., 2010. Analysis of fluid flow and heat transfer in a rib grit roughened surface solar air heater using CFD. Solar Energy, 84(3), 409-417.
[64] Boulemtafes-Boukadoum, A., & Benzaoui, A. J. E. P., 2014. CFD based analysis of heat transfer enhancement in solar air heater provided with transverse rectangular ribs. Energy Procedia, 50, 761-772.
[65] Singh, S., Singh, B., Hans, V. S., & Gill, R. S., 2015. CFD (computational fluid dynamics) investigation on Nusselt number and friction factor of solar air heater duct roughened with non-uniform cross-section transverse rib. Energy, 84, 509-517.
[66] Gawande,V.B., Dhoble,A.S., Zodpe,D.B., Chamoli,S., 2015b. Experimental and CFD based thermal performance prediction of solar air heater provided with right-angle triangular rib as artificial roughness. J. Braz. Soc. Mech. Sci. Eng. 38, 551–579.
[67] Singh, A., & Singh, S., 2017. CFD investigation on roughness pitch variation in non-uniform cross-section transverse rib roughness on Nusselt number and friction factor characteristics of solar air heater duct. Energy, 128, 109-127.
[68] Thakur, D. S., Khan, M. K., & Pathak, M., 2017. Performance evaluation of solar air heater with novel hyperbolic rib geometry. Renewable Energy, 105, 786-797.
[69] Kumar, A., Kumar, N., Kumar, S., & Maithani, R., 2023. Exergetic efficiency analysis of impingement jets integrated with internal conical ring roughened solar heat collector. Experimental Heat Transfer, 36(1), 75-95.
[70] A.M. Fadhil, J.M. Jalil, G.A. Bilal, Experimental and numerical investigation of solar air collector with phase change material in column obstruction, J. Energy Storage 79 (2024) 110066, https://doi.org/10.1016/j.est.2023.110066.
[71] S. Yadav and R. P. Saini, "Numerical investigation on the performance of a solar air heater using jet impingement with absorber plate," Solar Energy, vol. 208, pp. 236–248, Sep. 2020, doi: 10.1016/j.solener.2020.07.088.
[72] Das, S., Biswas, A., & Das, B., 2023. Parametric investigation on the thermo-hydraulic performance of a novel solar air heater design with conical protruded nozzle jet impingement. Applied Thermal Engineering, 219, 119583.
[73] J. Pal and S. K. Singal, "Numerical Analysis of Influence of Angle of Attack on the Performance of Solar Air Heater Having Cylindrical Jet Impingement Plate," in 2023 10th International Conference on Power and Energy Systems Engineering (CPESE), IEEE, Sep. 2023, pp. 346–351. doi: 10.1109/CPESE59653.2023.10303058.

[74] T. Rajaseenivasan, S. Ravi Prasanth, M. Salamon Antony, K. Srithar, Experimental investigation on the performance of an impinging jet solar air heater, Alexandria Eng. J. 56 (2017) 63–69, https://doi.org/10.1016/j.aej.2016.09.004.
[75] A. Soni, S.N. Singh, Experimental analysis of geometrical parameters on the performance of an inline jet plate solar air heater, Sol. Energy. 148 (2017) 149–156, https://doi.org/10.1016/j.solener.2017.03.081.
[76] R. Nadda, A. Kumar, R. Maithani, Developing heat transfer and friction loss in an impingement jets solar air heater with multiple arc protrusion obstacles, Sol. Energy. 158 (2017) 117–131, https://doi.org/10.1016/j.solener.2017.09.042.
[77] R. Nadda, R. Kumar, A. Kumar, R. Maithani, Optimization of single arc protrusion ribs parameters in solar air heater with impinging air jets based upon PSI approach, Therm. Sci. Eng. Prog. 7 (2018) 146–154, https://doi.org/10.1016/j. tsep.2018.05.008.
[78] R. Maithani, S. Sharma, A. Kumar, Thermo-hydraulic and exergy analysis of inclined impinging jets on absorber plate of solar air heater, Renew. Energy. 179 (2021) 84–95, https://doi.org/10.1016/j.renene.2021.07.013.
[79] M. Zukowski, Experimental investigations of thermal and flow characteristics of a novel microjet air solar heater, Appl. Energy. 142 (2015) 10–20, https://doi.org/ 10.1016/j.apenergy.2014.12.052.
[80] R. Chauhan, N.S. Thakur, Investigation of the thermohydraulic performance of impinging jet solar air heater, Energy. 68 (2014) 255–261, https://doi.org/ 10.1016/j.energy.2014.02.059.
[81] R. Chauhan, T. Singh, N.S. Thakur, A. Patnaik, Optimization of parameters in solar thermal collector provided with impinging air jets based upon preference selection index method, Renew. Energy. 99 (2016) 118–126, https://doi.org/10.1016/j. renene.2016.06.046.
[82] R. Chauhan, T. Singh, N. Kumar, A. Patnaik, N.S. Thakur, Experimental investigation and optimization of impinging jet solar thermal collector by Taguchi method, Appl. Therm. Eng. 116 (2017) 100–109, https://doi.org/10.1016/j. applthermaleng.2017.01.025.
[83] A.M. Aboghrara, B.T.H.T. Baharudin, M.A. Alghoul, N.M. Adam, A.A. Hairuddin, H.A. Hasan, Performance analysis of solar air heater with jet impingement on corrugated absorber plate, Case Stud, Therm. Eng. 10 (2017) 111–120, https://doi. org/10.1016/j.csite.2017.04.002.
[84] D. Singh, B. Premachandran, S. Kohli, Numerical Simulation of the Jet Impingement Cooling of a Circular Cylinder, Numerical Heat Transfer, Part A: Applications 64 (2) (2013) 153–185, https://doi.org/10.1080/ 10407782.2013.772869.
[85] Tobergte D.R. and Curtis, S. (2013) Detection, Estimation, and Modulation Theory. Journal of Chemical Information and Modeling, 53, 1689-1699.
[86] Thakur, D.S., Khan, M.K., Pathak, M., 2017. Solar air heater with hyperbolic ribs: 3D simulation with experimental validation. Renewable Energy 113, 357–368. https:// doi.org/10.1016/j.renene.2017.05.096.
[87] Singh S, Chaurasiya SK, Negi BS, Chander S, Nem´ s M, Negi S. Utilizing circular jet impingement to enhance thermal performance of solar air heater. Renew Energy 2020;154:1327–45. https://doi.org/10.1016/j.renene.2020.03.095.
[88] Holman, J.P., 2001. Analysis of experimental data. In Experimental Methods for Engineers, 7th ed.; McGraw Hill: Singapore, pp. 48–143.